

## Hydrosilylation

How to cite: *Angew. Chem. Int. Ed.* **2021**, *60*, 550–565

International Edition: doi.org/10.1002/anie.202008729

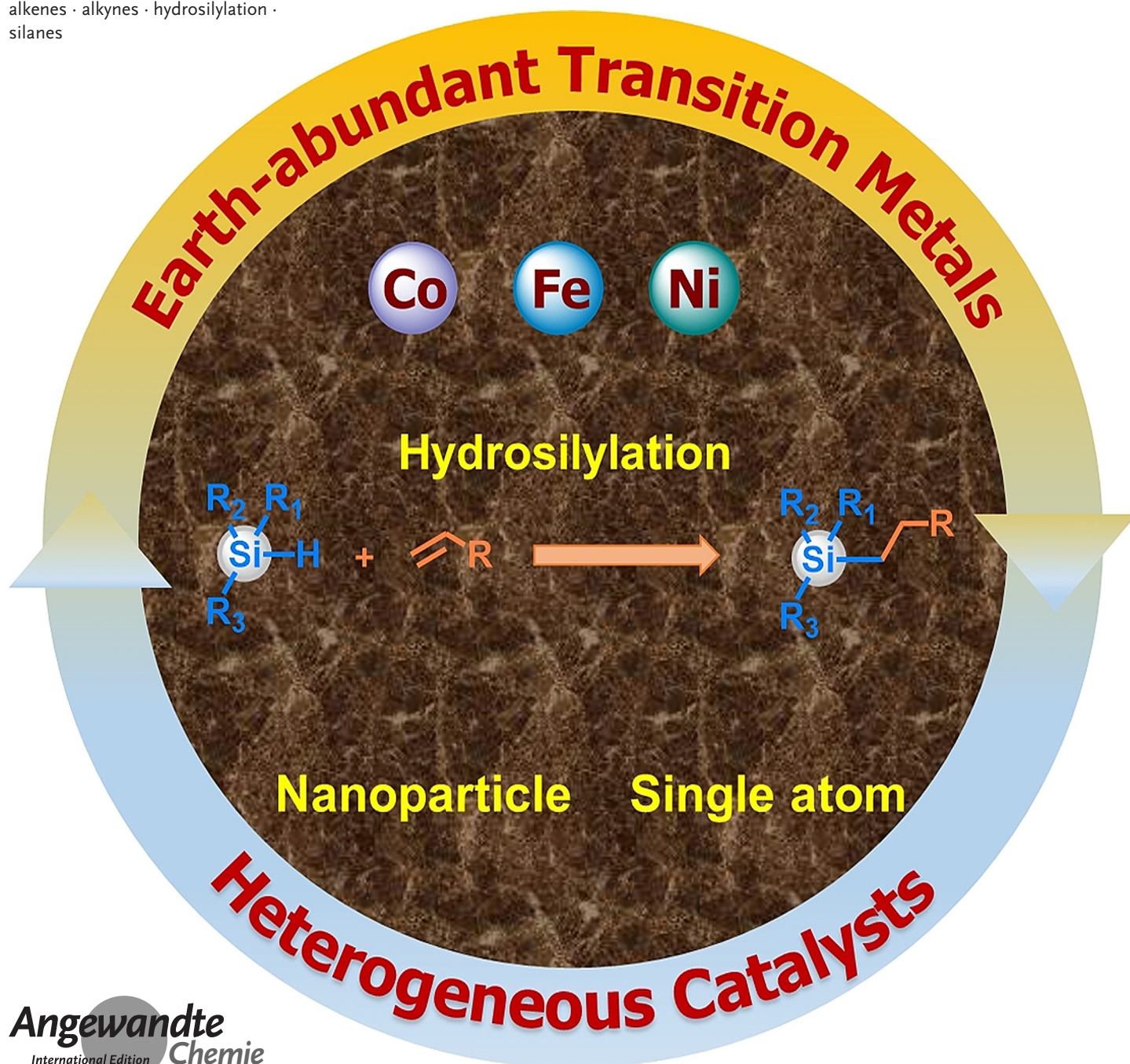
German Edition: doi.org/10.1002/ange.202008729

# Recent Advances in Catalytic Hydrosilylations: Developments beyond Traditional Platinum Catalysts

Leandro Duarte de Almeida<sup>+</sup>, Hongli Wang<sup>+</sup>, Kathrin Junge, Xinjiang Cui,<sup>\*</sup> and Matthias Beller<sup>\*</sup>

## Keywords:

alkenes · alkynes · hydrosilylation · silanes



**H**ydrosilylation reactions, which allow the addition of Si–H to C=C/C≡C bonds, are typically catalyzed by homogeneous noble metal catalysts (Pt, Rh, Ir, and Ru). Although excellent activity and selectivity can be obtained, the price, purification, and metal residues of these precious catalysts are problems in the silicone industry. Thus, a strong interest in more sustainable catalysts and for more economic processes exists. In this respect, recently disclosed hydrosilylations using catalysts based on earth-abundant transition metals, for example, Fe, Co, Ni, and Mn, and heterogeneous catalysts (supported nanoparticles and single-atom sites) are noteworthy. This minireview describes the recent advances in this field.

## 1. Introduction

Considering silicon as the second most abundant element on earth and the considerable number of organosilicon compounds used in our daily life, organosilicon chemistry is of significant importance for the development of more sustainable and greener chemistry. In general, organosilicon compounds are characterized by their stable and inert carbon–silicon bonds.<sup>[1–3]</sup> In particular, organosilanes, organosilyl halides, and the corresponding ethers are readily available and offer straightforward possibilities for versatile functionalizations. Compared to their ordinary pure carbon analogues, organosilicons have complementary physical properties, which make them attractive for a variety of industrial applications. Hence, organosilicon compounds are widely found in adhesives and coatings and used as oils, rubbers, and resins.<sup>[4]</sup>

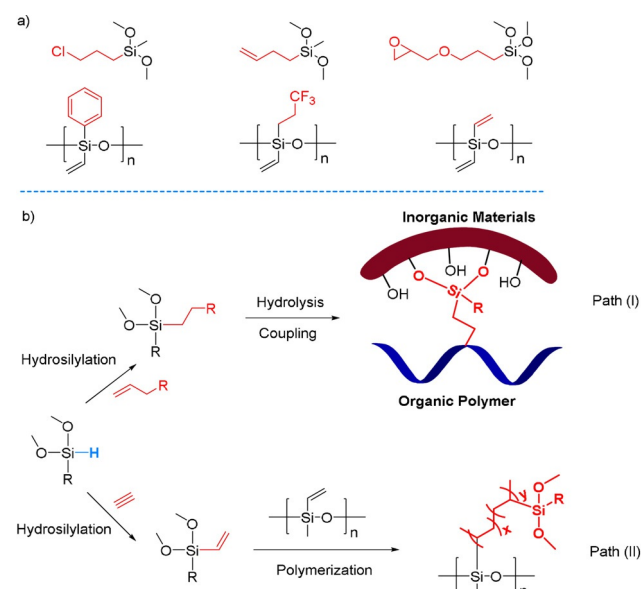


**Figure 1.** a) Selected functionalized silanes and silicone polymers; b) utilization of silane reagent: path (I): interfacial bonding by a silane coupling agent; path (II): crosslinking reaction between vinyl-containing silane and silicone polymers.

Among the different methods available for the creation of C–Si bonds, catalytic hydrosilylations allow the straightforward addition of silanes (Si–H) to multiple bonds, for example, olefins and alkynes.<sup>[5–15]</sup> These reactions are not only used on the laboratory scale, but have been also implemented in the chemical industry for the production of functional organosilicon compounds. In fact, they have been proven to be one of the most efficient reactions in the silicone industry. Theoretically, hydrosilylations are 100% atomic economic without generating other products or wastes.

Performing hydrosilylations with functionalized silanes (Figure 1 a) offers direct prospects to modify the properties of polymers or inorganic materials. For example, poly(dimethylsiloxane), an important kind of silicone rubber, can be functionalized by crosslinking with another vinyl silicon reagent (Figure 1 b).<sup>[16]</sup> Moreover, organosilicon compounds offer versatile properties as bonding or bridging agents in the preparation of composites from organic polymers and inorganic materials, for example, glass, minerals, and metal oxides.<sup>[17]</sup> Thus, apart from their importance for applications in the silicone industry, hydrosilylations are increasingly attractive for basic material sciences.<sup>[9,18–25]</sup>

Since the first hydrosilylation reaction appeared in the academic literature in 1947, platinum-based catalysts dominated this area.<sup>[26]</sup> Originally, the introduction of Speier's catalyst (H<sub>2</sub>PtCl<sub>6</sub>) was a major breakthrough. Later on, Karstedt made an important contribution to this area by developing a platinum(0) complex containing vinyl-siloxane ligands.<sup>[27]</sup> Today, this lipophilic complex represents an efficient benchmark catalyst in industrial hydrosilylation processes. Despite the efficiency of this system, obviously there are certain disadvantages of homogeneous Pt-based catalysts in some applications. For example, platinum complexes can be easily trapped in the product and it is difficult to recover them due to the viscous properties of the resulting

[\*] Dr. H. Wang,<sup>[†]</sup> Prof. X. Cui  
State Key Laboratory for Oxo Synthesis and Selective Oxidation  
Lanzhou Institute of Chemical Physics, Chinese Academy of Sciences  
No. 18, Tianshui Middle Road, Lanzhou, 730000 (China)  
E-mail: XinjiangCui@licp.cas.cn

M. Sc. L. D. de Almeida,<sup>[†]</sup> Dr. K. Junge, Prof. M. Beller  
Leibniz-Institute for Catalysis  
Albert-Einstein-Str. 29a, 18059 Rostock (Germany)  
E-mail: Matthias.Beller@catalysis.de

[†] These authors contributed equally to this work.

The ORCID identification number(s) for the author(s) of this article can be found under:  
<https://doi.org/10.1002/anie.202008729>.

© 2020 The Authors. Published by Wiley-VCH GmbH. This is an open access article under the terms of the Creative Commons Attribution Non-Commercial License, which permits use, distribution and reproduction in any medium, provided the original work is properly cited and is not used for commercial purposes.



products.<sup>[28–32]</sup> Notably, it was estimated that consumption of platinum accounts for up to 30% of the cost of silicones.<sup>[33]</sup> Hence, from an industrial point of view, the high price of platinum strongly motivates researchers to develop recyclable and less expensive catalysts to reduce the precious metal consumption.

The development and importance of hydrosilylation reactions has been discussed intensively in the scientific literature, and a number of comprehensive reviews, articles, and books were published mainly before 2015.<sup>[3,4,34]</sup> Since then, a variety of robust homogeneous catalysts with well-defined ligands have been developed.<sup>[35]</sup> More recently, also heterogeneous catalysts evolved for this process.<sup>[36]</sup> Interestingly, heterogeneous single-atom catalysts (SACs), which are considered to combine the advantages of molecular-defined and heterogeneous catalysis, were disclosed and displayed comparable activities and selectivities to their homogeneous counterparts.<sup>[37]</sup>



*Leandro Duarte de Almeida, born in Jundiaí (Brazil) in 1992, obtained his bachelor's and master's degrees at the Universidade Federal de Minas Gerais (Brazil). In 2018, he started his PhD at the same university under the direction of Prof. Patricia Alejandra Robles-Azocar with a research stay in Rostock at the Leibniz Institute of for Catalysis (Germany) supervised by Prof. Matthias Beller. His work is focused on valorization of terpenes and their derivatives using catalytic systems.*



*Hongli Wang was born in Shaanxi Province (China) in 1984. He obtained his PhD degree in 2013 at Lanzhou University, under the supervision of Prof. Yong-Min Liang and Prof. Shang-Dong Yang. From 2013–2015 he worked as a postdoctoral research fellow with Prof. Jin-Quan YuHe at Shanghai Institute of Organic Chemistry, CAS. He joined the faculty of Lanzhou Institute of Chemical Physics as an assistant research fellow in 2015 and was promoted to associate professor in 2019. His research focuses on catalytic synthesis of high value-added chemicals with C1 molecules.*



*Kathrin Junge, born in 1967 in northern Germany, received her PhD degree in Chemistry from the University of Rostock in 1997 working with Prof. E. Popowski. After a postdoctoral position in the Max-Planck group of Uwe Rosenthal, she joined the group led by Matthias Beller in 2000. Since 2008 she has been the group leader for sustainable redox reactions at LIKAT. Her current main research interest is the development of environmentally benign and efficient homogeneous and heterogeneous catalytic reactions based on inexpensive, non-precious metals.*

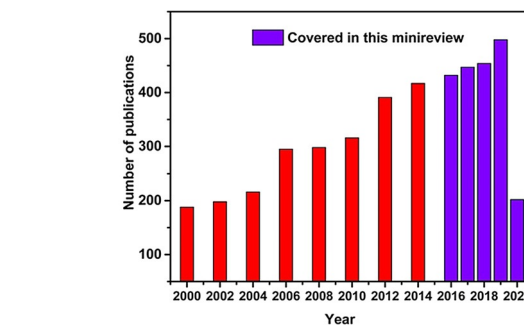


**Figure 2.** Number of publications using the term “hydrosilylation” from 2000 to May of 2020 according to the ISI Web of Science.

This minireview covers the most important catalyst developments from the past five years (Figure 2). To make it easy for the reader, it is organized according to catalyst developments into two sections: a) the use homogeneous non-noble metal complexes specifically Co, Fe, and Ni derivatives; b) the usage of recyclable heterogeneous catalysts focusing on supported noble/non-noble nanoparticles (NP) and single-atom catalysts. Finally, we will give indications for future progress in this field.

## 2. The Development of Homogeneous Non-noble Metal Catalysts

The replacement of traditional platinum-based catalysts in alkene hydrosilylations by more sustainable and economic



*Xinjiang Cui, born in China in 1984, obtained his PhD in 2013 supervised by Prof. Youquan Deng and Prof. Feng Shi at Lanzhou Institute of Chemical Physics (LICP), CAS. Then he worked one and half years at LICP as an assistant researcher. He conducted postdoctoral research at the Leibniz Institute for Catalysis with Prof. Matthias Beller (2014–2017) and at École Polytechnique Fédérale de Lausanne (EPFL) with Prof. Paul J. Dyson (2018–2019). In 2020, he returned to LICP and started his academic career independently as a full professor. His interests focus on the transformation of light chain hydrocarbons and the synthesis of fine chemicals with olefins by*

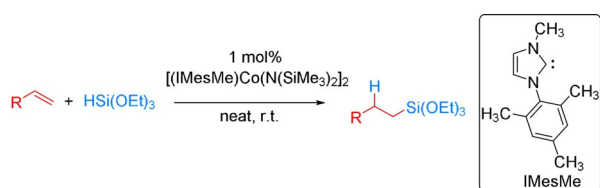


*Matthias Beller, born in Gudensberg (Germany) in 1962, obtained his PhD in 1989 working with Lutz F. Tietze at the University of Göttingen. After one year of postdoctoral research with Barry Sharpless at MIT (USA), he worked at Hoechst AG in Frankfurt (1991–1995) before he started his academic career at TU Munich. In 1998, he relocated to Rostock to head the Leibniz Institute for Catalysis. The research of his group focuses on applying homogeneous and heterogeneous catalysis for the synthesis of fine/bulk chemicals as well as energy technologies.*

metals is a long-standing goal of the silicone industry.<sup>[31,38–41]</sup> Following this goal, several molecularly defined catalysts based on earth-abundant metals (Fe, Co, Ni, et. al.) have been developed in the past decade.<sup>[5–7,9,13,42–46]</sup> Moreover, the regioselectivity can be controlled by modification of ligands leading to anti-Markovnikov or Markovnikov selective products. The resulting silane products are widely used as silicon fluids and silicon curing agents. Furthermore, the anti-Markovnikov silanes are also important moieties for life science applications.<sup>[47–49]</sup>

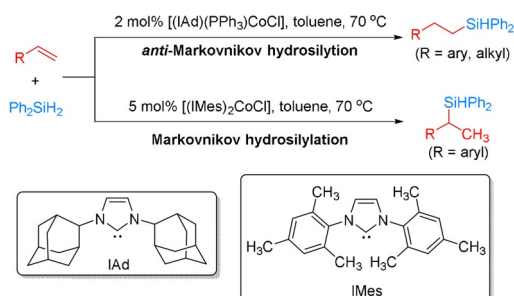
### 2.1. Catalysts with Monodentate Ligands

In 2017, Deng et al. reported cobalt N-heterocyclic carbene (NHC)-catalyzed anti-Markovnikov hydrosilylations of aliphatic alkenes with tertiary silanes (Scheme 1).<sup>[50]</sup> Specifically, they developed a cobalt(II) amide/NHC catalyst system, which facilitated the selective hydrosilylation of monosubstituted aliphatic alkenes with HSi(OEt)<sub>3</sub> to linear products in moderate to very high yields (42–98%). However, when highly reactive Ph<sub>3</sub>SiH was used with 1-octene, a lower yield of only 28% was observed. According to mechanistic studies Co-silyl intermediates are involved in the catalytic cycle with cobalt(I) species proposed as the active intermediates.



**Scheme 1.** Hydrosilylation of aliphatic alkenes with tertiary silanes using a cobalt-NHC catalyst.<sup>[50]</sup>

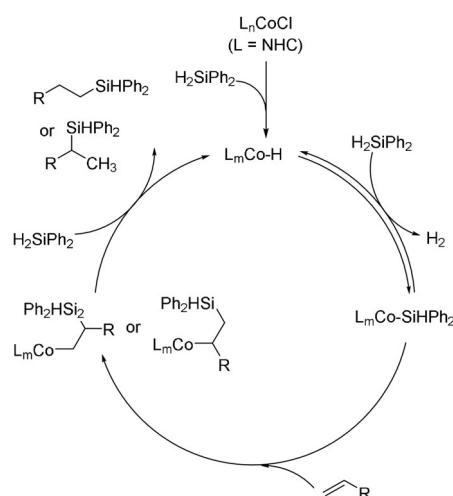
One year later, the same group disclosed that related Co<sup>I</sup>-NHC complexes such as [(IAd)(PPh<sub>3</sub>)CoCl] and [(IMes)<sub>2</sub>CoCl] displayed distinct performance in catalyzing the reaction of diverse alkenes with Ph<sub>2</sub>SiH<sub>2</sub> (Scheme 2).<sup>[51]</sup> Interestingly, [(IAd)(PPh<sub>3</sub>)CoCl] proved to be efficient in catalyzing anti-Markovnikov hydrosilylation of Ph<sub>2</sub>SiH<sub>2</sub> with both alkyl- and aryl-substituted alkenes, while [(IMes)<sub>2</sub>CoCl]



**Scheme 2.** Catalytic behavior of cobalt(I)-NHC complexes in the hydrosilylation of alkenes with diphenylsilane.<sup>[51]</sup>

promoted Markovnikov hydrosilylation of Ph<sub>2</sub>SiH<sub>2</sub> with aryl-substituted alkenes. The authors explain the changed catalytic performance by the different steric nature of the carbene ligands IAd vs. IMes.

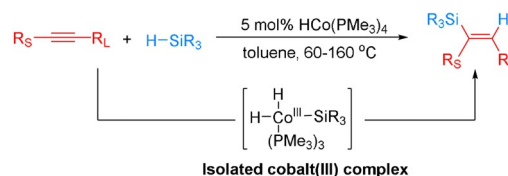
Here, mechanistic studies suggested that cobalt(I) silyl species are the key active species for the hydrosilylation process. On the basis of their results, a preliminary mechanism of this transformation was proposed (Scheme 3): Initial reaction of cobalt(I)-NHC chloride with Ph<sub>2</sub>SiH<sub>2</sub> gives a cobalt(I) hydride intermediate, which interacts with Ph<sub>2</sub>SiH<sub>2</sub> to form the corresponding cobalt(I) silyl intermediate and H<sub>2</sub>. Subsequent reaction of the cobalt(I) silyl intermediate with an alkene via migratory insertion forms a cobalt alkyl complex that further reacts with Ph<sub>2</sub>SiH<sub>2</sub> to give the desired hydrosilylation products and regenerates the active cobalt(I) silyl species for the next catalytic cycle.



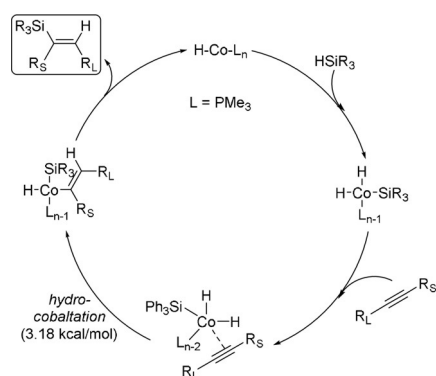
**Scheme 3.** Proposed catalytic cycle for the Co-NHC-catalyzed hydrosilylation.<sup>[51]</sup>

In 2016, Petit and colleagues described the HCo(PMe<sub>3</sub>)<sub>4</sub>-catalyzed highly regio- and stereoselective hydrosilylation of internal alkynes (Scheme 4).<sup>[52]</sup> The reaction was applied to a variety of hydrosilanes and symmetrical as well as unsymmetrical alkynes, giving in many cases a single hydrosilylation isomer in varying yields (19–96%). The authors suggested that the regio- and stereocontrol of the reaction is predominantly governed by steric features of the substrates.

According to mechanistic studies, dihydridocobalt species are most likely involved in this catalytic process (Scheme 5). Oxidative addition of the silane to a Co<sup>I</sup> hydride center forms



**Scheme 4.** HCo(PMe<sub>3</sub>)<sub>4</sub>-catalyzed highly regio- and stereoselective hydrosilylation of internal alkynes.<sup>[52]</sup>

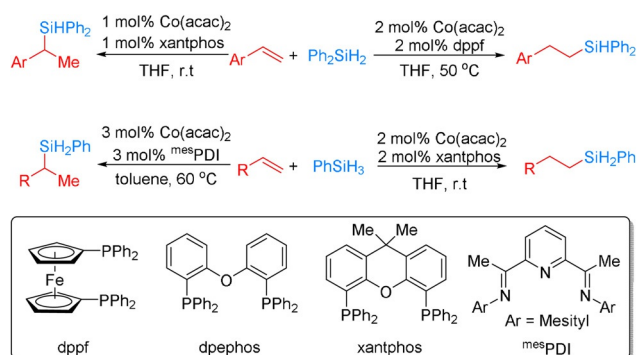


**Scheme 5.** Proposed mechanism for  $\text{HCo}(\text{PMe}_3)_4$ -catalyzed highly regio- and stereoselective hydrosilylation of internal alkynes.<sup>[52]</sup>

the dihydridocobalt(III) intermediate, which undergoes alkyne insertion into one of the Co–H bonds after coordination of the alkyne. Direct reductive elimination releases the vinylsilane as the major product with the observed regioselectivity and regenerates the catalytically active hydridocobalt(I) species.

## 2.2. Catalysts with Bidentate Ligands

In 2017, Wang et al. developed a regiodivergent cobalt-catalyzed hydrosilylation of alkenes by careful choice of ligands and hydrosilane substrates (Scheme 6).<sup>[53]</sup> More specifically, a  $\text{Co}(\text{acac})_2/\text{Xantphos}$  catalyst system showed excellent activity for Markovnikov hydrosilylation of styrene derivatives with  $\text{PhSiH}_3$ , whereas the  $\text{Co}(\text{acac})_2/\text{dppf}$  catalyst system facilitated the anti-Markovnikov hydrosilylation of styrene derivatives with  $\text{Ph}_2\text{SiH}_2$ . In contrast, utilizing aliphatic alkenes with  $\text{PhSiH}_3$ , in the presence of  $\text{Co}(\text{acac})_2/\text{mesPDI}$  as the catalyst, produced branched organosilanes in high yields (50%–98%) with high to excellent regioselectivities (b/l ratio: 91:9 to >99:1), while the corresponding linear products were obtained with  $\text{Co}(\text{acac})_2$  and  $\text{Xantphos}$ . Deuterium-labeling studies support the classic Chalk–Harrod mechanism with a Co–H intermediate resulting from oxidative addition of the silane to the metal center for the cobalt/



**Scheme 6.** Ligand- and silane-dependent cobalt-catalyzed regiodivergent hydrosilylation of vinylarenes and aliphatic alkenes.<sup>[53]</sup> acac = acetylacetonate.

bisphosphine system. Interestingly, a modified mechanistic proposal with Co–Si intermediates has been suggested for the cobalt/pyridine-2,6-diimine system.

Furthermore,  $\beta$ -diketiminato-based catalysts, such as the dimeric  $\beta$ -diketiminato manganese hydride (**Mn-1**) and the dimeric  $\beta$ -diketiminato magnesium hydride (**Mg-1**) in Figure 3, were also developed for anti-Markovnikov alkene hydrosilylation.<sup>[54,55]</sup> Using **Mn-1** as catalyst, aliphatic alkenes underwent anti-Markovnikov hydrosilylation to afford (*E*)- $\beta$ -vinylsilanes with 37–99% conversion, while the hydrosilylation of styrenes afforded  $\alpha$ -vinylsilanes with 19–99% conversion through Markovnikov hydrosilylation.

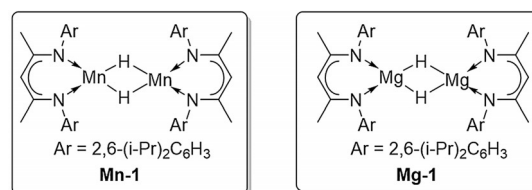
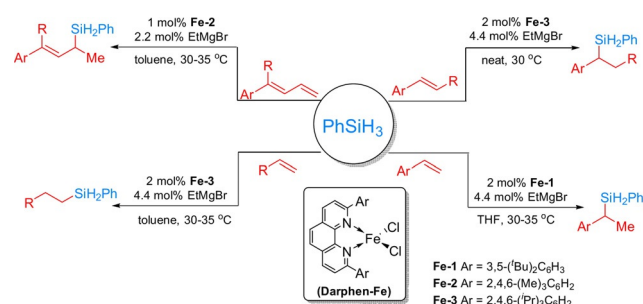


**Figure 3.** The structures of dimeric  $\beta$ -diketiminato manganese and magnesium hydride.<sup>[54,55]</sup>

In 2018, Zhu et al. described selective hydrosilylations of alkenes with Fe-based catalysts in the presence of 1,10-phenanthroline ligands (Scheme 7).<sup>[56]</sup> In particular, the combination of  $\text{FeCl}_2$  with 2,9-diaryl-1,10-phenanthroline ligands exhibited good reactivity and selectivity for hydrosilylation of both styrenes and aliphatic alkenes.

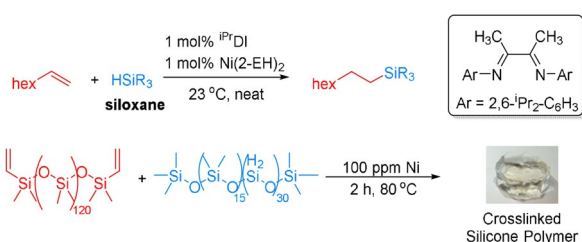


**Scheme 7.** Iron-catalyzed hydrosilylation of alkenes with phenylsilane.<sup>[56]</sup>

As shown in Scheme 7, **Fe-1** and **Fe-2** showed very high Markovnikov selectivity ( $\geq 98\%$ ) in the hydrosilylation of terminal styrenes, 1-substituted, and 1,1-disubstituted buta-1,3-dienes and led to the corresponding products in high yields (88–95%). However, in the presence of **Fe-3**, anti-Markovnikov products were obtained in the hydrosilylation of 1-alkyl ethylene derivatives in 72–98% yields. Kinetic isotope effect experiments and density functional theory (DFT) calculations suggest direct Si migration as the rate-determining step. Unfortunately, these iron catalyst systems seem to be limited to hydrosilylations with  $\text{PhSiH}_3$  and required Grignard reagents ( $\text{EtMgBr}$ ) for catalyst activation.



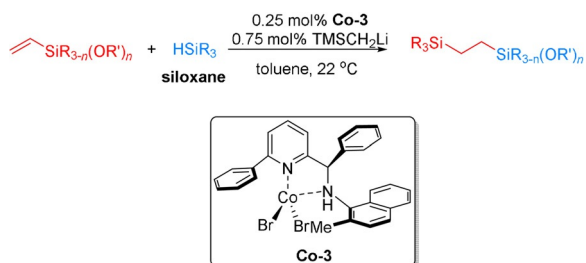
Compared to the hydrosilylations of simple alkenes with primary or secondary silanes (vide supra), hydrosilylation of alkenes or vinylsilanes with tertiary alkoxy- or siloxyhydrosilanes for silicone synthesis are considered more challenging from an industrial perspective. The resulting silicones represent industrially relevant fluids and curing materials. However, competitive hydrogenation of alkenes and alkynes can easily occur during the hydrosilylation process when the ligands are changed slightly. In this respect the work of Chirik and co-workers is notable. Here a nickel(II) bis(carboxylate) catalyst was used, which displayed high activity in the hydrosilylation of alkenes with a variety of industrially relevant tertiary alkoxy- and siloxy-substituted silanes. Under optimal conditions, selective anti-Markovnikov hydrosilylation of aliphatic alkenes with commercially relevant silanes and siloxanes was achieved in a practical manner (Scheme 8).<sup>[57]</sup>



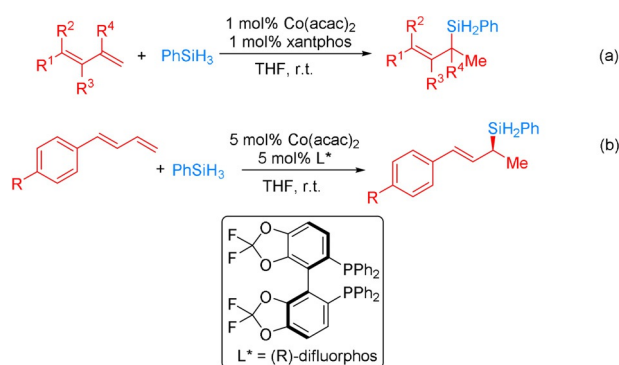
**Scheme 8.** Alkene hydrosilylation with  $\alpha$ -diimine nickel catalysts. 2-EH = 2-ethylhexanoate.<sup>[57]</sup>

In 2017, Lee and co-workers synthesized more than 25 cobalt-(aminomethyl)pyridine complexes and explored their catalytic performance for anti-Markovnikov hydrosilylations (Scheme 9).<sup>[58]</sup> With **Co-3** as the optimal catalyst system, various alkoxy(vinyl)silanes including mono-, di-, and triethoxy(vinyl)silanes and their corresponding methoxy derivatives reacted with alkoxy- or siloxyhydrosilanes to afford the desired anti-Markovnikov products in 70–99% yield with > 98% anti-Markovnikov selectivity.

Shortly thereafter, Ge and co-workers developed the highly selective cobalt-catalyzed stereoconvergent Markovnikov 1,2-hydrosilylation of conjugated dienes (Scheme 10a).<sup>[59]</sup> In the presence of 1 mol% of  $\text{Co}(\text{acac})_2$  and xantphos at room temperature, a wide range of conjugated *trans*-dienes encompassed aryl-substituted, alkyl-substituted, and multi-



**Scheme 9.** Cobalt-catalyzed anti-Markovnikov hydrosilylation of alkoxy- or siloxy(vinyl)silanes with alkoxy- or siloxyhydrosilanes.<sup>[58]</sup> TMS = trimethylsilyl.

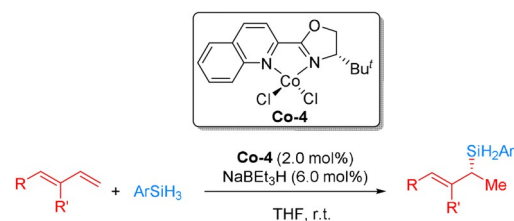


**Scheme 10.** Markovnikov 1,2-hydrosilylation of conjugated dienes: a) regioselective stereoconvergent and b) asymmetric variant.<sup>[59]</sup>

ple-substituted dienes reacted smoothly with  $\text{PhSiH}_3$  and  $\text{Ph}_2\text{SiH}_2$  affording the corresponding (*E*)-allylsilanes in 64–92% yield with excellent regioselectivities (*b/l* > 99:1). Furthermore, asymmetric Markovnikov 1,2-hydrosilylation of (*E*)-1-aryl-1,3-dienes with  $\text{PhSiH}_3$  in the presence of  $\text{Co}(\text{acac})_2$ /(*R*)-difluorophos proceeded smoothly to afford the desired products in 61–80% yield with good enantioselectivities (88:12–90:10 e.r.) (Scheme 10b). Mechanistic studies revealed that this stereoconvergence resulted from a  $\sigma$ - $\pi$ - $\sigma$  isomerization of an allylcobalt species generated by the 1,4-hydrometalation of (*Z*)-dienes. A Chalk–Harrod mechanism involving the 2,1-insertion of the terminal double bond of the diene into the  $\text{Co-H}$  bond was proposed.

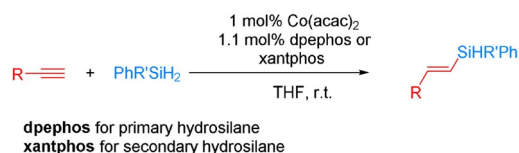
More recently, the Huang group developed a quinoline-oxazoline-based cobalt complex for the asymmetric 1,2-Markovnikov hydrosilylation of conjugated dienes with primary silanes (Scheme 11).<sup>[60]</sup> The *t*-Bu-substituted analogue (QuinOxtBu) $\text{CoCl}_2$  (**Co-4**) was identified as an effective catalyst for the highly regio- and enantioselective 1,2-Markovnikov hydrosilylation of various conjugate dienes bearing aryl/alkyl substituents with  $\text{PhSiH}_3$ , furnishing chiral allyl silanes in high yields with high regioselectivity (up to > 99:1) and enantioselectivity (up to 96% *ee*) in the presence of  $\text{NaBEt}_3\text{H}$ .  $\text{Ph}_2\text{SiH}_2$  was less reactive than  $\text{PhSiH}_3$ , while tertiary silanes ( $\text{Et}_3\text{SiH}$  and  $(\text{EtO})_2\text{MeSiH}$ ) are unreactive. A modified Chalk–Harrod mechanism involving the 1,2-insertion of the terminal double bond of the diene into the  $\text{Co-Si}$  bond is assumed.

Apart from olefins and dienes, the hydrosilylation of alkynes has been investigated with non-noble metal com-



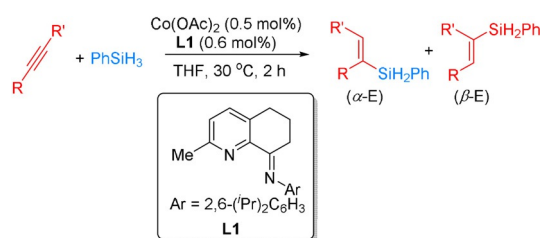
**Scheme 11.** The asymmetric 1,2-Markovnikov hydrosilylation of conjugated dienes with primary silanes using pyridine/quinoline-oxazoline chiral  $\text{Co}^{\text{II}}$  dichloride complexes.<sup>[60]</sup>

plexes bearing bidentate ligands.<sup>[61]</sup> In this context, Ge et al. reported a Co-catalyzed anti-Markovnikov hydrosilylation of terminal alkynes with both primary and secondary hydrosilanes PhR'SiH<sub>2</sub> (Scheme 12).<sup>[62]</sup> With Co(acac)<sub>2</sub> and dpephos or xantphos as ligands, a broad range of alkynes containing either aromatic or aliphatic substituents underwent this hydrosilylation reaction smoothly at room temperature to afford (*E*)-vinylsilanes in 59–91% yield with high regioselectivity ((*E*)-β:α 89:11 to 99:1).



**Scheme 12.** The anti-Markovnikov hydrosilylation of terminal alkynes using Co(acac)<sub>2</sub> and bisphosphine ligands.<sup>[62]</sup>

Complementary to that work, Jin and co-workers developed an efficient cobalt-catalyzed Markovnikov-selective hydrosilylation of alkynes using bidentate CImPy ligands such as **L1** in 2019 (Scheme 13).<sup>[63]</sup> The hydrosilylation of aromatic and aliphatic alkynes with primary and secondary silanes proceeded well to form the corresponding products in 36–98% yield with moderate to high regioselectivities (α/β 63:37 to 99:1). The comparably high catalytic activity enabled by the CImPy ligand is ascribed to the high stereoelectronic tunability and rigid environment, which suppresses the deactivation of the catalyst.



**Scheme 13.** Cobalt-catalyzed Markovnikov-selective hydrosilylation of alkynes using bidentate CImPy ligands such as **L1**.<sup>[63]</sup>

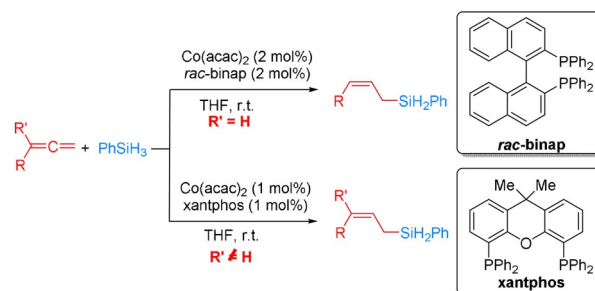
Recently, Zhu and co-workers described also an Fe-catalyzed dihydrosilylation of aliphatic terminal alkynes and primary silanes for the synthesis of geminal bis(silanes) (Scheme 14).<sup>[64]</sup> Reactions of PhSiH<sub>3</sub> and *n*-C<sub>12</sub>H<sub>25</sub>SiH<sub>3</sub> with a range of aliphatic terminal alkynes generated the corre-



**Scheme 14.** Iron-catalyzed dihydrosilylation of alkynes for the synthesis of geminal bis(silanes).<sup>[64]</sup>

sponding geminal bis(silanes) as the sole hydrosilylation products in 85–95% yield. This method allowed the efficient synthesis of previously unreported geminal bis(silanes) with secondary silyl groups. Mechanistic studies demonstrated that the reaction proceeds via two iron-catalyzed hydrosilylation reactions, the first generating β-(*E*)-vinylsilanes and the second producing geminal bis(silanes).

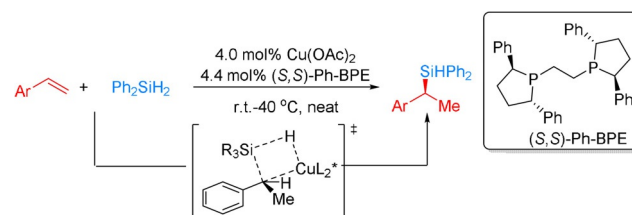
Based on their work on alkyne hydrosilylation, Ge and co-workers also disclosed a highly regio- and stereoselective hydrosilylation of allenes by employing a bench-stable catalyst system consisting of Co(acac)<sub>2</sub> and binap or xantphos ligands (Scheme 15).<sup>[65]</sup> Allyl- or vinylsilanes can be easily



**Scheme 15.** Cobalt-catalyzed (*Z*)-selective allene hydrosilylation.<sup>[65]</sup>

prepared by selective hydrosilylation of allenes with hydrosilanes in the presence of transition metal catalysts. The major difficulty in these reactions is to control the regio- and stereoselectivity preventing the formation of different vinyl- and allylsilane products. Here, a variety of mono- and disubstituted terminal allenes reacted with primary and secondary hydrosilanes to produce the desired disubstituted (*Z*)-allylsilanes in high yields (57–95%) with excellent stereoselectivity (*Z*:*E* = 99:1). Unfortunately, hydrosilylation of allenes did not occur when tertiary hydrosilanes were used. The regio- and stereocontrol of the reaction is explained by the steric repulsion between the substituent on the allyl group and the ligand of the cobalt catalyst.

Another elegant example of asymmetric hydrosilylation was presented by Buchwald and co-workers in 2017. They demonstrated an enantioselective Cu–H catalyzed Markovnikov hydrosilylation of vinylarenes and associated vinyl heterocycles with Ph<sub>2</sub>SiH<sub>2</sub> (Scheme 16).<sup>[66]</sup> These reactions gave bench-stable silanes and chiral alcohol derivatives in 61–89% yield with good to excellent enantioselectivity (70–98% *ee*).

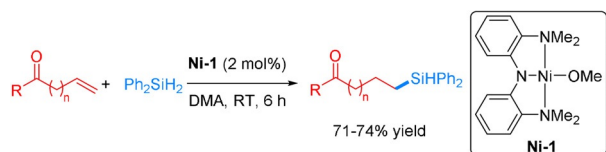


**Scheme 16.** Copper hydride-catalyzed asymmetric Markovnikov hydrosilylation of vinylarenes and vinyl heterocycles.<sup>[66]</sup>

### 2.3. Catalysts with Pincer Ligands

In the past two decades, catalysts with so-called pincer ligands have been extensively exploited for all kind of catalytic reactions, including hydrosilylations. In general, the corresponding complexes contain tridentate ligands, which bind to the metal center with three adjacent coplanar sites in a meridional configuration. Often pincer ligands have a central,  $\sigma$ -donating moiety that contains two side donor groups, typically either amino- or phosphinomethyl groups in *ortho*-position. Advantages of pincer complexes are their high thermal stability and well-defined reactivity with remaining coordination sites. In this section, recent studies on hydrosilylation using pincer catalysts will be discussed.

As an early example of alkene hydrosilylations, Chirik and co-workers used a nickel complex bearing a bis-(amino)amide NNN-pincer ligand. Their work was inspired by a related iron pincer catalyst, which, however, tolerated no carbonyl groups in the reaction.<sup>[67]</sup> Hydrosilylation of 1-octene with  $\text{Ph}_2\text{SiH}_2$  using 0.025 mol % of **Ni-1** achieved a 98% conversion in only 3 minutes, thus resulting in an impressive TOF of  $83\,000\text{ h}^{-1}$ . **Ni-1** was capable of efficiently converting differently substituted alkenes and cyclic alkenes with up to 94% yield. Interestingly, selective hydrosilylations of alkenes containing ketones and aldehydes groups were successfully conducted with yields from 71–74% (Scheme 17). In these reactions Ni hydride species are assumed to be potential intermediates.<sup>[6]</sup>

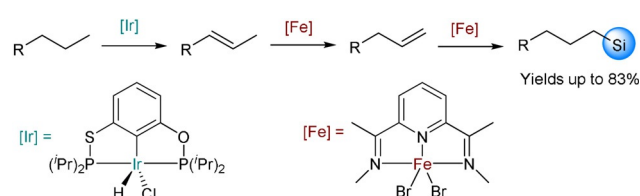


**Scheme 17.** Ni-catalyzed hydrosilylation of olefins containing carbonyl groups.<sup>[67]</sup> DMA = dimethylacetamide.

In general, low-valent Fe pincer complexes are known to be more unstable and difficult than iron(II/III) complexes. With this in mind, Thomas and co-workers prepared a series of  $\text{Fe}^{\text{II}}$  NNN-pincer complexes bearing Cl, Br, and OTf as counterions. Activation of such higher valent complexes was possible using tertiary amines at room temperature. Thus, in the presence of  $(i\text{Pr})_2\text{NEt}$  the Fe-pincer catalyst bearing OTf exhibited the best activity for the hydrosilylation of 1-octene with  $\text{PhSiH}_3$ , achieving 95% yield for the anti-Markovnikov product. This behavior explained by the fact that the ion/counterion bond strength of Fe-halides is stronger than that of Fe-OTf. With exception of nitro and nitrile groups, a broad scope of substituents was tolerated in the presence of this catalyst system, including carbonyl groups.<sup>[69]</sup>

An interesting one-pot cascade-like approach for alkane dehydrogenation/isomerization/hydrosilylation yielding terminal silanes was developed using a dual iridium/iron pincer catalytic system. Here, initially 1-octane is dehydrogenated in the presence of 1 mol % iridium catalyst and 1.2 mol % of  $\text{NaO}^t\text{Bu}$  at  $200^\circ\text{C}$ . For the isomerization/hydrosilylation

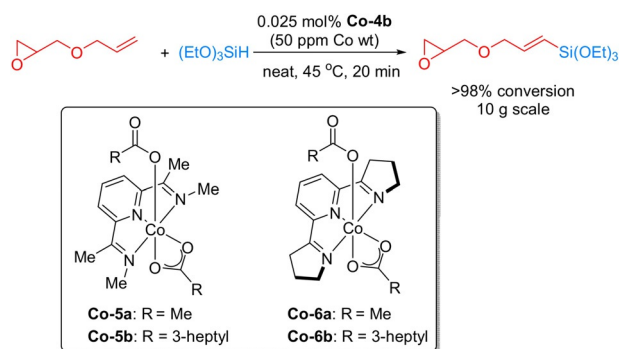
reactions, anti-Markovnikov products were obtained (67% yield) in the presence of 10 mol % of Fe-NNN pincer catalyst and 20 mol % of  $\text{NaHBEt}_3$  (Scheme 18). Control experiments revealed that the iridium catalyst played no role in the tandem isomerization/hydrosilylation reaction. Notably, the iron-catalyzed alkene hydrosilylation occurred with a high reaction rate, thus inhibiting reversible isomerization of the alkene.<sup>[68]</sup>



**Scheme 18.** One-pot dehydrogenation, isomerization and hydrosilylation catalyzed by iridium and iron pincer catalysts.<sup>[68]</sup>

The application of pincer ligands with less hindered imine groups favored hydrosilylation instead of dehydrogenative hydrosilylation of olefins.<sup>[7]</sup> In this context, Chirik and co-workers developed a Co-NNN pincer catalyst derived from **Co-5a** for hydrosilylations. The catalyst bearing a  $\text{CH}_2\text{SiMe}_3$  group showed high activity for 1-octene hydrosilylation with  $\text{HSi}(\text{OEt})_3$  at room temperature. Unfortunately, this catalyst is not bench-stable. Hence, more stable complexes **Co-5b** and **Co-6b** were prepared as catalysts by ligand modification. These stable catalysts exhibited excellent activity for hydrosilylations with alkoxy silanes. As an example, the hydrosilylation of sensitive allyl glycidyl ether was successfully conducted in the presence of **Co-6b** on a 10 g scale with 98% yield for the trialkoxysilane product, which finds widespread applications in industry (Scheme 19).<sup>[70]</sup>

Apart from olefins and alkynes, the hydrosilylation of 1,3- and 1,4-dienes was studied in the presence of **Co-5**. Thus, an anti-Markovnikov hydrosilylation of (*E*)-1,3-dodecadiene with phenylsilane occurred selectively. The following activity trend was observed for substituents on the pincer framework: 2,4,6-tri-Me < 2,6-di-Et < 2,6-di-*i*Pr. With this catalytic system, primary and secondary silanes ( $\text{PhSiH}_3$ ,  $\text{PhMeSiH}_2$ , and

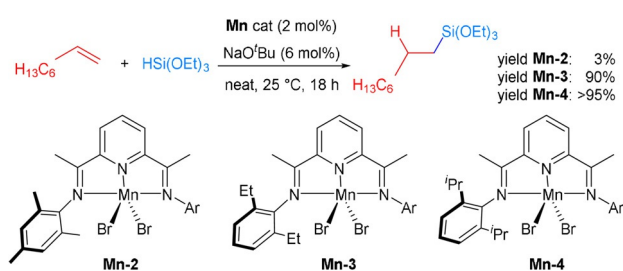


**Scheme 19.** Hydrosilylation of allyl glycidyl ether using a Co pincer catalyst.<sup>[70]</sup>



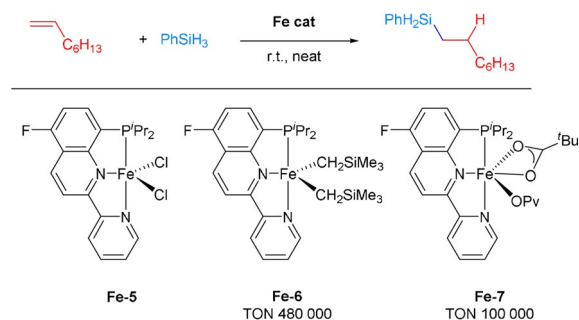
$\text{Ph}_2\text{SiH}_2$ ) were successfully converted into the desired anti-Markovnikov products in up to 92% yield, while tertiary silanes showed no activity for hydrosilylation, but instead led to hydrogenation of the corresponding dienes.<sup>[72]</sup>

Recently, manganese complexes including pincer ligands have become relatively popular in homogeneous catalysis.<sup>[73]</sup> Nevertheless, the use of such complexes for hydrosilylations of alkenes is still quite rare. As an exception several Mn-NNN pincer complexes (**Mn-2** to **Mn-4**) were used for hydrosilylation of terminal alkenes. These catalysts displayed excellent regioselectivity for a broad scope of alkenes and silanes, yielding the corresponding products up to 95% with >99% regioselectivity in the presence of  $\text{NaO}^t\text{Bu}$ . Apparently, the increased steric bulk of the ligand is favorable for this transformation. Hence, **Mn-4** led to higher hydrosilylation yields, which was also proven for the hydrosilylation of 1-octene with  $\text{HSi}(\text{OEt})_3$  in a gram-scale reaction (Scheme 20).<sup>[71]</sup>



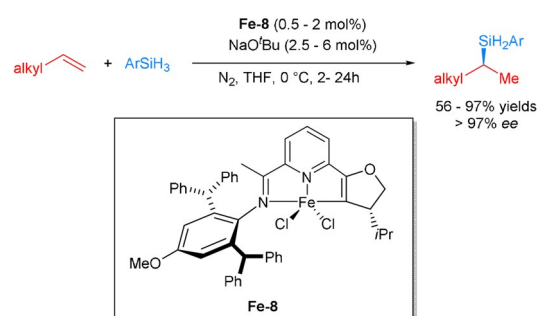
**Scheme 20.** Manganese-catalyzed alkene hydrosilylation.<sup>[71]</sup>

In 2019, a series of quinoline-derived Fe-PNN pincer complexes (**Fe-5** to **Fe-7**) were prepared, aiming for a bench-stable, activator- and solvent-free non-noble metal catalyst system (Scheme 21). In the presence of stoichiometric amounts of  $\text{LiCH}_2\text{SiMe}_3$  and  $\text{KO}^i\text{Piv}$ , **Fe-5** can be transformed to **Fe-6** and **Fe-7**, which are active catalysts for the hydrosilylation under base-free conditions. Using 1-octene and  $\text{PhSiH}_3$  as starting materials, **Fe-6** and **Fe-7** displayed excellent catalytic performance affording TONs of 480 000 and 100 000, respectively. Interestingly, **Fe-7** proved to be stable under air exposure, while **Fe-6** immediately decomposed upon air exposition. It was confirmed that Fe-H species, which are believed to be the active intermediates in the catalytic cycle, were produced in the presence of **Fe-6** and  $\text{PhSiH}_3$ .<sup>[74]</sup>



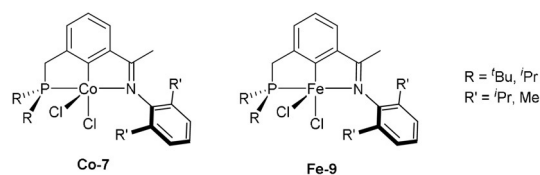
**Scheme 21.** Iron pincer-catalyzed 1-octene hydrosilylation.<sup>[74]</sup>

While pyridyl-derived NNN and quinoline-derived PNN pincer complexes favored the formation of the hydrosilylation products from aliphatic olefins (vide supra),<sup>[75,76]</sup> Lu and co-workers demonstrated a Markovnikov (enantio)selective hydrosilylation of terminal alkenes using different Fe-PNN pincer catalysts (**Fe-8**). In their elegant studies, they investigated a series of pyridine-based ligands with different oxazoline and imino substituents. An increased steric bulk of the imino group not only increased the selectivity of the hydrosilylation, but also improved the regio- and enantioselectivity. Comparing diverse oxazoline moieties, the *i*-Pr-substituted one exhibited better activity than that with Me and *t*Bu groups. Under optimal conditions, alkenes bearing bioactive molecules, such as naproxen, ibuprofen, and desloratadine, gave the desired products in a highly enantioselective manner in 91%, 97% and 88% yield, respectively. Moreover, an experiment with 1,5-hexadiene with 2.4 equiv of  $\text{PhSiH}_3$  provided the disilylated product in 90% yield with 96/4 branched/linear ratio and 97% *ee* (Scheme 22). With respect to asymmetric catalysis this development is noteworthy because it allows highly enantioselective functionalization of plain aliphatic olefins without any additional coordination sites.<sup>[77]</sup>



**Scheme 22.** Iron-catalyzed enantioselective Markovnikov hydrosilylation of alkenes.<sup>[77]</sup>

Compared to most known pincer ligands, phosphinite-iminopyridine ligands can be easily decomposed due to P-O bond cleavage.<sup>[9]</sup> Obviously, related phosphino-iminopyridine (PNN) ligands are more stable and have been explored with respect to their steric hindrance (Scheme 23). More specifically, **Fe-9** and **Co-7** pincer catalysts were prepared for regioselective Markovnikov alkene hydrosilylations. Interestingly, in the hydrosilylation of 1-octene with  $\text{PhSiH}_3$ , the Markovnikov product was mainly obtained using **Fe-9**, while the anti-Markovnikov was the major one in the presence of

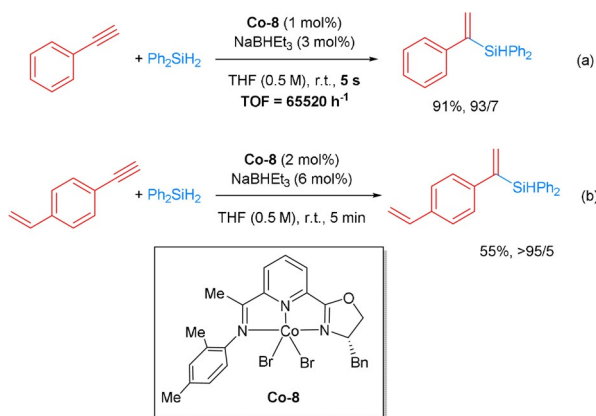


**Scheme 23.** Cobalt and iron PNN pincer catalysts used in alkene hydrosilylations.<sup>[78]</sup>

**Co-7.** The different product formation with the use of **Co-7** was ascribed to a different silyl migration mechanism involving a Co<sup>I</sup>-silyl intermediate. Ligand screening experiments revealed increased activity with the bulkier ligand for **Co-9**, whereas the less bulky ligand was more active for **Co-7**.<sup>[78]</sup>

The pincer catalysts also exhibited high activities in the selective hydrosilylation of alkynes.<sup>[79,80]</sup> In 2016, Lu and co-workers described an improved sequential hydrosilylation/asymmetric hydrogenation of terminal phenylalkynes to obtain chiral silanes using chiral Co-NNN pincer catalysts. After detailed investigations of the steric bulk of substituents on the pincer ligand, **Co-8** was identified as the optimal complex, which exhibited excellent catalytic performance for hydrosilylations of phenylacetylenes with Ph<sub>2</sub>SiH<sub>2</sub> with up to 91% yield and >99% *ee*. Mechanistic studies revealed that cobalt-hydride species are intermediates in this hydrosilylation reaction.<sup>[81]</sup> Notably, the hydrosilylations of phenylacetylenes proceeded extremely fast. In fact, a reaction with Ph<sub>2</sub>SiH<sub>2</sub> using 1 mol% of **Co-8** was completed in 5 seconds, which corresponds formally to a TOF of 65 000 h<sup>-1</sup> (Scheme 24 a). When the hydrosilylation of 4-vinylphenylacetylene was performed, a chemoselective reaction for the alkyne moiety was observed, although in lower yield (Scheme 24 b).<sup>[81]</sup> Later on, sequential double hydrosilylation of aliphatic alkynes to yield highly enantioenriched gem-bis(silyl)alkanes was achieved by the same group. Both experimental results and DFT calculations were analyzed to understand the reaction mechanism. It was shown that the highly enantioselective synthesis of gem-bis(silyl)alkanes is a result of the sequential asymmetric double 1,1-hydrosilylation of aliphatic alkynes in the presence of CoBr<sub>2</sub>·Xantphos, and CoBr<sub>2</sub>·OIP (OIP = oxazoline-iminopyridine).<sup>[82]</sup>

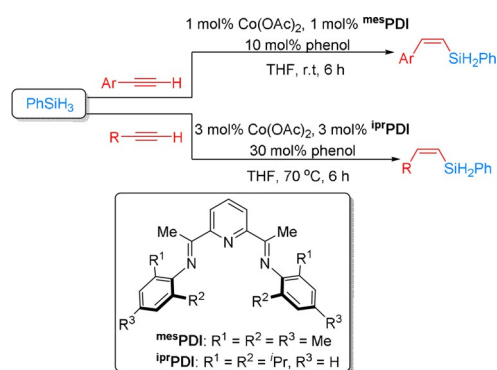
Moreover, asymmetric hydrosilylation of unsymmetric alkynes with dihydrosilanes producing silicon-stereogenic vinylhydrosilanes was realized with high regio- and enantioselectivity by Co-NNN catalysts. More specifically, Huang and co-workers reported the Markovnikov hydrosilylation of terminal alkynes with diphenylsilane in the presence of pyridine-bis(oxazoline) Co catalysts. Later on, the same group described alkyne hydrosilylations with prochiral dihydrosilanes in the presence of the same kind of cobalt/pyridine-



**Scheme 24.** Cobalt pincer complex-catalyzed alkyne hydrosilylation.<sup>[81]</sup>

bis(oxazoline)) complex producing Markovnikov silanes with up to 99% selectivity.<sup>[83,84]</sup>

In 2017, a series of cobalt pyridine-2,6-diimine complexes were prepared and tested for the *Z*-selective hydrosilylation of terminal alkynes with PhSiH<sub>3</sub>. In this work the less sterically hindered ligands favored the formation of  $\alpha$ -vinylsilanes, while (*Z*)- $\beta$ -vinylsilanes were preferred using <sup>mes</sup>PDI and <sup>ipr</sup>PDI. This behavior was attributed to the accessibility of the respective cobalt center. A broad range of alkynes including phenylacetylene and aliphatic alkynes were successfully converted to the desired products with *Z/E* ratios higher than 91:9 (Scheme 25). However, highly reactive nitro and aldehyde substituents were not tolerated. Moreover, aliphatic alcohol and carboxylic acid moieties inhibited the reaction.<sup>[85]</sup>



**Scheme 25.** Cobalt-catalyzed *Z*-selective hydrosilylation of terminal alkynes.<sup>[85]</sup>

### 3. Recyclable Heterogeneous Catalysts

In classical liquid-phase reactions, heterogeneous catalysts are more easily recycled than homogeneous ones. Although this advantage is also also holds for many catalytic hydrosilylations,<sup>[31,86]</sup> in a number of (industrial) cases, the corresponding products are either highly viscous or even polymers. In such cases, the practical benefit of a heterogeneous material is less obvious. Here, instead, the avoidance of (costly) ligands might be the main driver to search for heterogeneous catalysts. For this reason, an increasing number of heterogeneous catalysts have been explored in recent years. In this section, heterogeneous catalysts based on supported nanoparticles, including so-called supported single-atom catalysts, fabricated by different processes and their applications in hydrosilylation will be emphasized.

#### 3.1. Precious Metal Catalysts

##### 3.1.1. Pt Nanoparticle Catalysts

For a long time, the molecularly defined Karstedt complex has been regarded as the state-of-the-art catalyst for hydrosilylation reactions. Thus, also several attempts were made to immobilize this complex or derivatives on different supports.

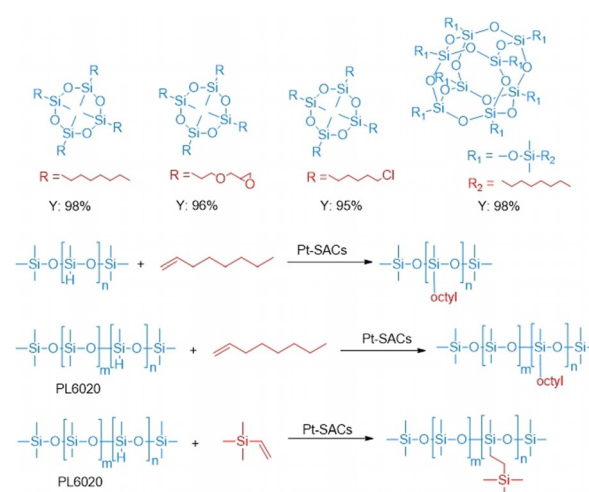
For example, a silica-supported Karstedt complex, which displayed initial high activity, was first prepared in 2003. However, for this material poor catalytic performance was observed after several reuses due to its low stability. Since then, other heterogeneous Pt catalysts have been broadly investigated.<sup>[87]</sup> In 2017, a mesostructured silica framework was used as a support where Pt nanoparticles (NPs) were embedded into walls of the silica matrix. The resulting material exhibited excellent catalyst turnover numbers of  $\text{TON} = 10^5$  for the hydrosilylation of 1-octene with polymethylhydrosiloxane (PMHS). Due to the physical trapping of the Pt NPs in the silica framework, no Pt leaching was observed after recycling.<sup>[88]</sup>

$\text{Pt}^0$  NPs were also embedded in a modified silica xerogel (SiliaCatPt(0)), which is obtained by sol-gel polycondensation of organosilanes. The resulting catalyst has a uniform spherical morphology and proved to be highly active and selective for a broad scope of olefins. However, the activity decreased sharply to 65% after the fourth cycle, probably caused by the slight size increase of Pt NPs.<sup>[89]</sup> To obtain effective catalyst separation from liquid silicone products, magnetic silica particles ( $\text{Fe}_3\text{O}_4@/\text{SiO}_2$ ) were used as support. After the material was modified by addition of ethylenediaminetetraacetic acid (EDTA) or diethylenetriaminepentaacetic acid (DTPA) and immobilization of Pt, the resulting catalysts displayed good activity even for the isomerization-hydrosilylation of internal alkenes.<sup>[90]</sup>

Recently, a graphene-supported platinum catalyst was synthesized using electrostatic adsorption techniques with solventless microwave irradiation. Using this special method, additional defects or holes in graphene are formed and simultaneously small Pt nanoparticles are stabilized with an average diameter of 6.8 nm. The resulting catalyst material displayed a superior efficiency in the hydrosilylation of 1,1,1,3,5,5,5-heptamethyltrisiloxane (MDM) and 1-octene, leading to a TON of  $9.4 \times 10^6$  which was tenfold higher than that obtained by the parent Karstedt catalyst ( $0.9 \times 10^6$ ).<sup>[36]</sup>

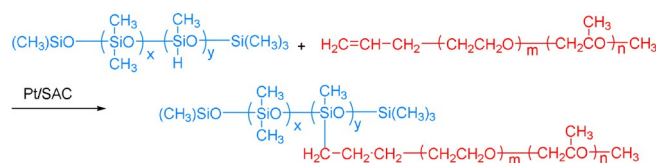
### 3.1.2. Pt Single-Atom Catalysts (Pt SACs)

Although several supported Pt nanoparticles were developed for catalytic hydrosilylations (vide supra), in some cases poor recyclability caused by leaching was observed. This was attributed to the weak binding of Pt particles to the support. Complementary to materials based on supported nanoparticles, single-atom catalysis provides a new concept to prepare materials with isolated metal centers, which are stabilized by neighboring sites of the support. In 2017, a Pt single-atom catalyst was synthesized by impregnation of platinum salts on aluminum oxide nanorods. The resulting Pt-SAC was applied for the selective hydrosilylation of all kinds of terminal olefins and exhibited excellent activity comparable to the original Karstedt system (Scheme 26). Interestingly, this Pt-SAC displayed also high stability, which is explained by the strong binding of the individual Pt atoms to their neighboring oxygen atoms.<sup>[37]</sup> Later on, superparamagnetic  $\text{Fe}_3\text{O}_4$ - $\text{SiO}_2$  core-shell nanoparticles (NPs) were used as the support in Pt single-atom catalysts. The material was easily separated from high-viscosity products by applying a magnetic field (Scheme 27).



**Scheme 26.** Pt SACs used for the selective hydrosilylation of various alkenes.<sup>[37]</sup>

Notably, the Pt loading decreased from 1.5% to 1.26% after four cycles.<sup>[91]</sup> Furthermore, a partially charged Pt single-atom catalyst was fabricated on the surface of anatase  $\text{TiO}_2$  ( $\text{Pt}_1^{\delta+}/\text{TiO}_2$ ) by an electrostatic-induction ion exchange. DFT calculations explained the excellent catalytic performance of this material by the intrinsic nature of partially charged  $\text{Pt}(\delta+)$  atoms on  $\text{TiO}_2$ . The authors also concluded that the lower oxidation state of Pt is favorable for the desired transformation compared to platinum in higher oxidation states (II or IV).<sup>[92]</sup>



**Scheme 27.** Pt-SAC for hydrosilylation.<sup>[91]</sup>

In order to prevent metal agglomeration in SACs, the metal loading is often (very) low. Recently, an interesting material was disclosed which contains isolated Pt single atoms in a dense distribution. It was successfully synthesized by the  $\text{NaCO}_3$ -assisted one-pot pyrolysis of an EDTA-Pt complex on N-doped graphene (Pt-ISA/NG in Figure 4). Here, the Pt centers are coordinated to N species instead of O. The Pt-ISA/NG exhibited microstructure and morphology features typical for atomically thin 2D graphene-like analogues, with a specific surface area of  $1892 \text{ m}^2 \text{ g}^{-1}$  and 5.3 wt% Pt loading. Pt-ISA/NG displayed high selectivity, activity, and stability for anti-Markovnikov hydrosilylation of different terminal alkenes with silanes under mild conditions.<sup>[93]</sup>

In the case of Pt NPs and SACs, the leaching of the metal is an important aspect, which has to be avoided. Although the average loss of Pt was calculated to be several ppm in each round of reaction, the involvement of the leached Pt could not be excluded because the hydrosilylation easily initiated even



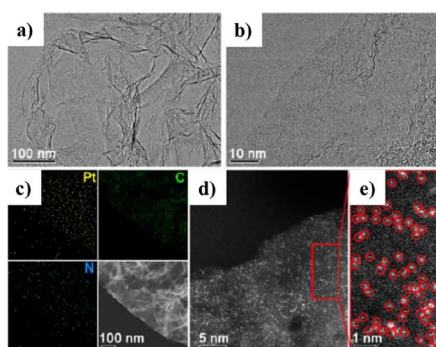


**Figure 4.** Characterization of the Pt-ISA/NG catalyst: a) Typical transmission electron microscopy (TEM) image. b) High-resolution TEM (HRTEM) image. c) Energy-dispersive X-ray (EDX) mapping. d,e) Aberration-corrected high-angle annular dark-field scanning transmission electron microscopy (AC-HAADFSTEM) image and corresponding enlarged view. Reproduced with permission.<sup>[93]</sup> Copyright 2018, American Chemical Society.

by a ppm amounts of Pt. Moreover, the leaching problem leads to difficulties in mechanistic studies and contamination in the final silicon products.

### 3.1.3. Other Precious Metal Catalysts

Apart from platinum, other precious metal catalysts based on Au, Rh, and Ru have been reported for hydrosilylation reactions of olefins and related substrates. For example, highly regioselective alkene hydrosilylation is possible in the presence of gold nanoparticles on TiO<sub>2</sub> or Al<sub>2</sub>O<sub>3</sub>. In this case, ionic gold(I) species at the interface between the nanoparticles and the support were suggested as the active sites.<sup>[86]</sup>

Recently, Rh<sup>I</sup> complexes were co-immobilized with tertiary amines on the surface of SiO<sub>2</sub> (referred to as SiO<sub>2</sub>/Rh-NEt<sub>2</sub>). SiO<sub>2</sub>/Rh-NEt<sub>2</sub> exhibited excellent turnover numbers for the hydrosilylation of olefins with a wide range of substrates. The good catalytic performance was ascribed to the electron donation from amine groups to the Rh complex, which promotes both the oxidative addition and insertion steps during the hydrosilylation cycle.<sup>[94]</sup>

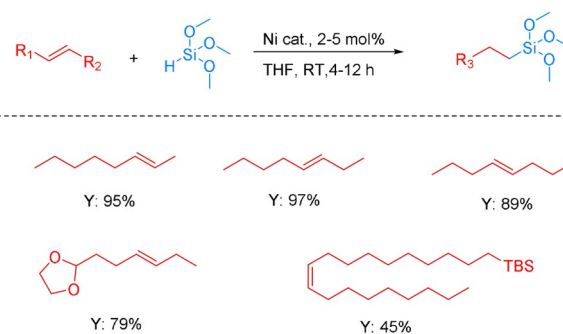
Despite significant progress with heterogeneous catalysts using supported noble metals, the hydrosilylation of internal alkenes is still challenging. In this context, Prieto and co-workers demonstrated an interesting isomerization–hydrosilylation of internal alkenes. Very recently, they successfully developed a process involving tandem catalysis by Rh and Ru single-atom catalysts on CeO<sub>2</sub>. When these two SACs were combined in a single reaction, a synergetic effect was observed and high selectivity was obtained for the hydrosilylation of different internal alkenes with Et<sub>3</sub>SiH. DFT calculations ascribed the observed selectivity to differences in the binding strength of the alkene substrate where the single Ru atoms bind more strongly than the Rh counterparts.<sup>[95]</sup>

## 3.2. Non-Precious Metal Catalysts

### 3.2.1. Nickel-Based Heterogeneous Catalysts

In 2016, Hu and co-workers developed the first nickel nanoparticle catalyst, which is able to catalyze alkene hydrosilylation with tertiary silanes. In this case, nickel nanoparticles with an average size of 3.5 nm were formed in situ using a particular nickel alkoxide potassium salt (Ni(OtBu)<sub>2</sub>·xKCl). Interestingly, the resulting Ni nanoparticles displayed high activity not only in the hydrosilylation of terminal alkenes with high anti-Markovnikov selectivity, but also in the tandem isomerization–hydrosilylation of *cis* and *trans* internal alkenes in high yields (Scheme 28). Consequently, this non-precious metal catalyst is able to synthesize a single terminal alkyl silane from a mixture of different internal and terminal olefin isomers.<sup>[96]</sup> Later on, other isolated Ni nanoparticles stabilized by *n*-octylsilane were prepared by decomposition of Ni(COD)<sub>2</sub> (COD = cycloocta-1,5-diene) in toluene under 4 bar of H<sub>2</sub>. The resulting Ni colloid (Ni<sub>3</sub>Si<sub>2</sub>) consists of very small nanoparticles 1.2 nm in diameter. However, with this system only moderate conversion (70%) and low selectivity (30%) were achieved for the model hydrosilylation of triethoxyvinylsilane with triethoxysilane.<sup>[97]</sup>

In 2019, a novel supported nickel catalyst was prepared whereby isolated nickel centers were anchored on a metal–organic framework (MOF) carrier. The single metal sites are considered to be stabilized by the hydroxyl groups from the MOF forming the active centers. Using this catalyst, the hydrosilylation of *n*-octene and diphenylsilane was carried out on a 150 mmol scale under mild conditions with high conversion and selectivity.<sup>[98]</sup> Furthermore, isolated Ni centers stabilized by heterogeneous ligands have been applied for hydrosilylation reactions very recently. In this latter case, a porous organic polymer containing Xantphos (POP-Xantphos) moieties was used to stabilize the isolated nickel centers. The prepared Ni-POP-Xantphos catalyst demonstrated high regio- and stereoselectivity in the hydrosilylation of alkynes. The obtained selectivity was considered to be controlled by the microporous structure of POP-Xantphos.<sup>[99]</sup>



**Scheme 28.** Ni-catalyzed tandem isomerization–hydrosilylation of internal alkenes.<sup>[96]</sup>

### 3.2.2. Cobalt-Based Heterogeneous Catalysts

Comparable to the Ni-POP-Xantphos catalyst (vide supra), isolated Co sites were coordinated with a POP-PPh<sub>3</sub> ligand (Co-POP-PPh<sub>3</sub>). The resultant Co-POP-PPh<sub>3</sub> material catalyzed the hydrosilylation of alkynes with PhSiH<sub>3</sub> with high regio- and stereoselectivity. Moreover, the reusability of Co-POP-PPh<sub>3</sub> was tested in a continuous-flow system. Even after several rounds of recycling only little loss of activity and selectivity was observed.<sup>[100]</sup> Recently, also Co/TiO<sub>2</sub> was synthesized where the cobalt ions were doped onto the TiO<sub>2</sub> surface. After hydrogen treatment, CoTiO<sub>3</sub> species were formed, which exhibited excellent catalytic performance for the hydrosilylation of various alkenes under neat conditions. Importantly, the CoTiO<sub>3</sub> species were not leached after recycling due to the strong interaction between Co and TiO<sub>2</sub>, leading to high stability and reusability.<sup>[101]</sup>

### 3.2.3. Iron-Based Heterogeneous Catalysts

In 2016, Lin and co-workers reported an iron-based catalyst for several hydrosilylation reactions of terminal alkenes using a two-dimensional (2D) metal-organic layer (MOL) carrier. The synthesized MOL was composed of [Hf<sub>6</sub>O<sub>4</sub>(OH)<sub>4</sub>(HCO<sub>2</sub>)<sub>6</sub>] as secondary building units (SBUs) and benzene-1,3,5-tribenzoate (BTB) as bridging ligands. After connecting the MOL with 4'-(4-benzoate)-(2,2',2''-terpyridine)-5,5''-dicarboxylate (TPY), the resulting MOL-TPY was used to immobilize iron centers, affording single-site solid catalysts (Fe-MOL-TPY, Figure 5). A variety of terminal alkenes were converted to the corresponding alkyl silanes with PhSiH<sub>3</sub> in high yields. Fe-MOL-TPY is free from diffusional constraints, leading to high activity and reusability.<sup>[102]</sup>

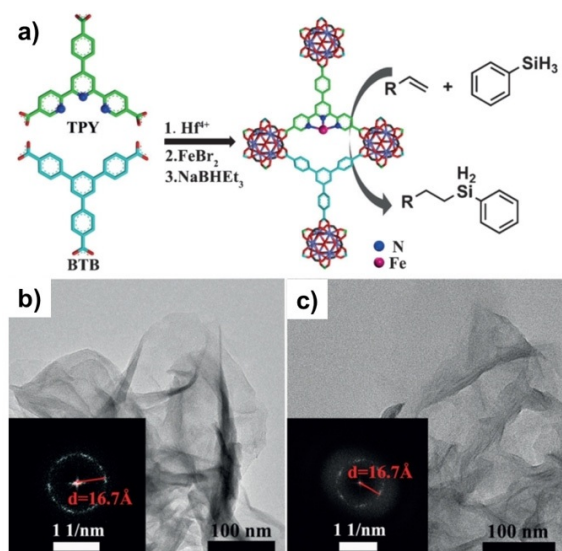


**Figure 5.** a) Preparation of the MOL catalyst Fe-TPY-MOL. b, c) HRTEM and FFT images of Fe-TPY-MOL before (b) and after catalysis (c). Reproduced with permission.<sup>[102]</sup> Copyright 2016, Wiley-VCH.

In addition to Fe-SACs, iron oxide nanoparticles (Fe<sub>2</sub>O<sub>3</sub>) were synthesized in a practical way using iron(III) acetylacetonate as the precursor and *N,N*-dimethylformamide (DMF) as both the reducing and protecting agent. The DMF-stabilized Fe<sub>2</sub>O<sub>3</sub> nanoparticles were monodispersed in the solvent and showed high catalytic activity for the hydrosilylation of alkenes in the absence of any additives. Furthermore, the colloidal catalyst can be recycled by simple extraction with a hexane/DMF system for fifth run.<sup>[103]</sup>

### 3.2.4. Bimetallic Heterogeneous Catalysts

Bimetallic nanoparticles can exhibit exclusive catalytic performances, distinct from those of monometallic NPs, due to their unique electronic states and structures. As an example, Li and co-workers developed a bimetallic catalyst by immobilizing Pt<sub>1</sub>Ni<sub>1</sub> nanoparticles on the surface of nitrogen-doped carbon (NC). The Pt<sub>1</sub>Ni<sub>1</sub>/NC-1000 catalyst, which was obtained by pyrolysis of metal-organic frameworks at 1000 °C, displayed the highest catalytic performance for the hydrosilylation benchmark reaction of 1-octene with HSi(OEt)<sub>3</sub>. Characterizations revealed a high graphitization degree, which should favor a stronger charge transfer between the NC support and Pt<sub>1</sub>Ni<sub>1</sub>, forming more positively charged Pt centers. These charged Pt species possibly lead to the higher catalytic activity.<sup>[105]</sup>

In 2017, Cai and co-workers developed an efficient and recyclable Pd<sub>1</sub>Cu<sub>2</sub> bimetallic catalyst. The Pd<sub>1</sub>Cu<sub>2</sub> NPs were supported on SiO<sub>2</sub> and exhibited superior activity and selectivity toward the hydrosilylation of internal and terminal alkynes. The catalytic performance is improved by the ultrasmall size (2.8 nm) and the high dispersion of the Pd-Cu nanoparticles as well as the enrichment of Pd on the catalyst surface (Figure 6).<sup>[104]</sup>

Finally, heterogeneous catalysts using bimetallic materials have been used for hydrosilylations of alkynes. Here, Shishido and co-workers reported the use of Pd-Au bimetallic NPs at ambient temperature. After careful screening of supports and

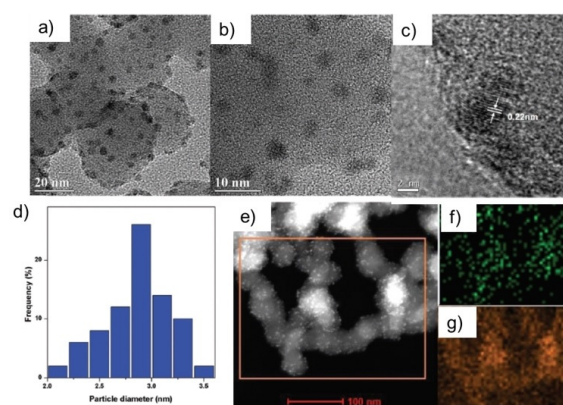


**Figure 6.** Characterization of the Pd<sub>1</sub>Cu<sub>2</sub>/SiO<sub>2</sub> catalyst: a, b) TEM images. c) High-resolution TEM (HRTEM) image of the Pd<sub>1</sub>Cu<sub>2</sub>/SiO<sub>2</sub> catalyst. d) Size distribution of Pd<sub>1</sub>Cu<sub>2</sub> bimetallic nanoparticles. e) High-angle annular dark field (HAADF) STEM image of Pd<sub>1</sub>Cu<sub>2</sub>/SiO<sub>2</sub>. f, g) EDS elemental maps for Pd (f) and Cu (g). Reproduced with permission.<sup>[104]</sup> Copyright 2017, The Royal Society of Chemistry.

metal ratios, Pd<sub>1</sub>Au<sub>5</sub>/Nb<sub>2</sub>O<sub>5</sub> catalyst was identified as the most active catalyst for the hydrosilylation of alkynes with complete *trans*-configured products. High activity was observed for the catalyst with a relatively low Pd/Au ratio of 1:5, which is in accord with the isolated single Pd atoms characterized in Pd<sub>1</sub>Au<sub>5</sub>/Nb<sub>2</sub>O<sub>5</sub>.<sup>[106]</sup>

#### 4. Challenges and Perspectives

The catalytic addition of silanes to olefins and alkynes (hydrosilylation reaction) continues to attract significant interest among academic and industrial chemists. In fact, this methodology remains a key technology for innovations in the silicone industry. For the advancement of this field, the development of new and improved catalysts is a prerequisite. In this respect, the present report discusses briefly actual developments of nonclassical homogeneous and heterogeneous catalysts for hydrosilylation reactions. In addition to molecularly defined non-noble metal catalysts, also recently discovered heterogeneous catalysts such as supported noble/non-noble NPs and single-atom catalysts are discussed. Considering all these achievements, what are the major challenges in research on catalytic hydrosilylation reactions in the coming decade?

Apart from few examples, most of the academic developments—which are by no means scientifically very interesting—are far from being relevant for industry and real-world applications. This is because of the model reactions used, the reaction conditions applied, and the substrates investigated. We believe there is an enormous innovation potential, if the gap between academic and industrial research can be bridged more efficiently.

In the development of new powerful homogeneous catalysts, the complexity of the ligand part is often underestimated, sometimes fully neglected. Obviously, an ideal catalytic system not only constitutes an available, less toxic metal center, for example, iron or manganese, but also inexpensive, stable, and modular ligands. Looking at recently disclosed ligand scaffolds, a number can be synthesized only on small scale under special conditions, for example, in a glovebox. Especially, for non-noble metal catalysts it is still a challenge to develop practical ligands.

The use of heterogeneous catalysts for hydrosilylation reactions is a fascinating, growing scientific area. Here, the detailed understanding of the structural features that control the regio- and stereoselectivity of a given catalyst is still missing. Clearly, such knowledge is the basis for any rational catalyst development. Here, the use of heterogeneous SACs with a limited and defined number of atomic species, where the metal centers are spatially isolated from each other, might give new impetus. Furthermore, the combination of supported (multi)metallic NPs in the presence or absence of ligands will offer alternative solutions for directing regio- and stereoselectivities of hydrosilylations.

#### Acknowledgements

We acknowledge financial support by National Key Research and Development Program of China (2017YFA0403103), Chinese Academy of Sciences, Key Research Program of Frontier Sciences of CAS (QYZDJ-SSW-SLH051), Light of West China, and Youth Innovation Promotion Association (2019409). We also acknowledge the State of Mecklenburg-Western Pomerania, the Federal State of Germany (BMBF), and the EU (ERC Advanced Grant NoNaCat) for financial support. Coordenação de Aperfeiçoamento de Pessoal de Nível Superior—Brasil (CAPES)—Finance Code 001. Open access funding enabled and organized by Projekt DEAL.

#### Conflict of interest

The authors declare no conflict of interest.

- [1] E. G. Rochow, *Silicon and Silicones: About Stone-age Tools, Antique Pottery, Modern Ceramics, Computers, Space Materials and How They All Got That Way*, Springer, Berlin, **1987**.
- [2] R. Murugavel, A. Voigt, M. G. Walawalkar, H. W. Roesky, *Chem. Rev.* **1996**, *96*, 2205–2236.
- [3] I. Fleming, A. Barbero, D. Walter, *Chem. Rev.* **1997**, *97*, 2063–2192.
- [4] B. Marciniak, *Coord. Chem. Rev.* **2005**, *249*, 2374–2390.
- [5] C. Chen, M. B. Hecht, A. Kavara, W. W. Brennessel, B. Q. Mercado, D. J. Weix, P. L. Holland, *J. Am. Chem. Soc.* **2015**, *137*, 13244–13247.
- [6] I. Buslov, J. Becouse, S. Mazza, M. Montandon-Clerc, X. Hu, *Angew. Chem. Int. Ed.* **2015**, *54*, 14523–14526; *Angew. Chem.* **2015**, *127*, 14731–14734.
- [7] C. C. H. Atienza, T. N. Diao, K. J. Weller, S. A. Nye, K. M. Lewis, J. G. P. Delis, J. L. Boyer, A. K. Roy, P. J. Chirik, *J. Am. Chem. Soc.* **2014**, *136*, 12108–12118.
- [8] A. Simonneau, M. Oestreich, *Angew. Chem. Int. Ed.* **2013**, *52*, 11905–11907; *Angew. Chem.* **2013**, *125*, 12121–12124.
- [9] D. J. Peng, Y. L. Zhang, X. Y. Du, L. Zhang, X. B. Leng, M. D. Walter, Z. Huang, *J. Am. Chem. Soc.* **2013**, *135*, 19154–19166.
- [10] M. E. Fasulo, M. C. Lipke, T. D. Tilley, *Chem. Sci.* **2013**, *4*, 3882–3887.
- [11] A. M. Tondreau, C. C. H. Atienza, K. J. Weller, S. A. Nye, K. M. Lewis, J. G. P. Delis, P. J. Chirik, *Science* **2012**, *335*, 567–570.
- [12] E. Abinet, T. P. Spaniol, J. Okuda, *Chem. Asian J.* **2011**, *6*, 389–391.
- [13] J. Y. Wu, B. N. Stanzl, T. Ritter, *J. Am. Chem. Soc.* **2010**, *132*, 13214–13216.
- [14] S. Díez-González, S. P. Nolan, *Acc. Chem. Res.* **2008**, *41*, 349–358.
- [15] F. Buch, H. Brettar, S. Harder, *Angew. Chem. Int. Ed.* **2006**, *45*, 2741–2745; *Angew. Chem.* **2006**, *118*, 2807–2811.
- [16] A. K. Roy, *Adv. Organomet. Chem.* **2008**, *55*, 1–59.
- [17] P. E. Plueddemann, *Silane Coupling Agents*, Plenum Press, New York, **1991**.
- [18] Z. Y. Zhao, Y. X. Nie, R. H. Tang, G. W. Yin, J. Cao, Z. Xu, Y. M. Cui, Z. J. Zheng, L. W. Xu, *ACS Catal.* **2019**, *9*, 9110–9116.
- [19] Y. Q. Zhang, N. Funken, P. Winterscheid, A. Gansauer, *Angew. Chem. Int. Ed.* **2015**, *54*, 6931–6934; *Angew. Chem.* **2015**, *127*, 7035–7038.



- [20] A. L. Liberman-Martin, R. G. Bergman, T. D. Tilley, *J. Am. Chem. Soc.* **2015**, *137*, 5328–5331.
- [21] T. Bleith, H. Wadepohl, L. H. Gade, *J. Am. Chem. Soc.* **2015**, *137*, 2456–2459.
- [22] Z. Y. Yang, M. Iqbal, A. R. Dobbie, J. G. C. Veinot, *J. Am. Chem. Soc.* **2013**, *135*, 17595–17601.
- [23] C. D. F. Königs, H. F. T. Klare, M. Oestreich, *Angew. Chem. Int. Ed.* **2013**, *52*, 10076–10079; *Angew. Chem.* **2013**, *125*, 10260–10263.
- [24] M. Stoelzel, C. Prasang, S. Inoue, S. Enthaler, M. Driess, *Angew. Chem. Int. Ed.* **2012**, *51*, 399–403; *Angew. Chem.* **2012**, *124*, 411–415.
- [25] K. Osakada, *Angew. Chem. Int. Ed.* **2011**, *50*, 3845–3846; *Angew. Chem.* **2011**, *123*, 3929–3930.
- [26] L. H. Sommer, E. W. Pietrusza, F. C. Whitmore, *J. Am. Chem. Soc.* **1947**, *69*, 188.
- [27] B. D. Karstedt, General Electric Company, US3775452A, **1973**.
- [28] I. E. Markó, S. Stérin, O. Buisine, G. Mignani, P. Branlard, B. Tinant, J. P. Declercq, *Science* **2002**, *298*, 204–206.
- [29] I. E. Markó, S. Stérin, O. Buisine, G. Berthon, G. Michaud, B. Tinant, J. P. Declercq, *Adv. Synth. Catal.* **2004**, *346*, 1429–1434.
- [30] P. Gigler, M. Drees, K. Riener, B. Bechlers, W. A. Herrmann, F. E. Kuhn, *J. Catal.* **2012**, *295*, 1–14.
- [31] B. Marciniec, K. Posala, I. Kownacki, M. Kubicki, R. Taylor, *ChemCatChem* **2012**, *4*, 1935–1937.
- [32] M. Igarashi, T. Kobayashi, K. Sato, W. Ando, T. Matsumoto, S. Shimada, M. Hara, H. Uchida, *J. Organomet. Chem.* **2013**, *725*, 54–59.
- [33] M. Y. Hu, P. He, T. Z. Qiao, W. Sun, W. T. Li, J. Lian, J. H. Li, S. F. Zhu, *J. Am. Chem. Soc.* **2020**, *142*, 16894–16902.
- [34] D. Troegel, J. Stohrer, *Coord. Chem. Rev.* **2011**, *255*, 1440–1459.
- [35] J. V. Obligacion, P. J. Chirik, *Nat. Rev. Chem.* **2018**, *2*, 15–34.
- [36] C. J. Kong, S. E. Gilliland, B. R. Clark, B. F. Gupton, *Chem. Commun.* **2018**, *54*, 13343–13346.
- [37] X. Cui, K. Junge, X. Dai, C. Kreyenschulte, M. M. Pohl, S. Wohlrab, F. Shi, A. Bruckner, M. Beller, *ACS Cent. Sci.* **2017**, *3*, 580–585.
- [38] O. Buisine, G. Berthon-Gelloz, J. F. Briere, S. Sterin, G. Mignani, P. Branlard, B. Tinant, J. P. Declercq, I. E. Marko, *Chem. Commun.* **2005**, 3856–3858.
- [39] C. M. Downing, H. H. Kung, *Catal. Commun.* **2011**, *12*, 1166–1169.
- [40] J. J. Dunsford, K. J. Cavell, B. Kariuki, *J. Organomet. Chem.* **2011**, *696*, 188–194.
- [41] L. Ortega-Moreno, R. Peloso, C. Maya, A. Suarez, E. Carmona, *Chem. Commun.* **2015**, *51*, 17008–17011.
- [42] L. Benítez Junquera, M. C. Puerta, P. Valerga, *Organometallics* **2012**, *31*, 2175–2183.
- [43] K. Kamata, A. Suzuki, Y. Nakai, H. Nakazawa, *Organometallics* **2012**, *31*, 3825–3828.
- [44] M. I. Lipschutz, T. D. Tilley, *Chem. Commun.* **2012**, *48*, 7146–7148.
- [45] M. D. Greenhalgh, D. J. Frank, S. P. Thomas, *Adv. Synth. Catal.* **2014**, *356*, 584–590.
- [46] V. Srinivas, Y. Nakajima, W. Ando, K. Sato, S. Shimada, *Catal. Sci. Technol.* **2015**, *5*, 2081–2084.
- [47] E. Rémond, C. Martin, J. Martinez, F. Cavalier, *Chem. Rev.* **2016**, *116*, 11654–11684.
- [48] E. Langkopf, D. Schinzer, *Chem. Rev.* **1995**, *95*, 1375–1408.
- [49] T. A. Blumenkopf, L. E. Overman, *Chem. Rev.* **1986**, *86*, 857–873.
- [50] Y. Liu, L. Deng, *J. Am. Chem. Soc.* **2017**, *139*, 1798–1801.
- [51] Y. F. Gao, L. J. Wang, L. Deng, *ACS Catal.* **2018**, *8*, 9637–9646.
- [52] A. Rivera-Hernández, B. J. Fallon, S. Ventre, C. Simon, M. H. Tremblay, G. Gontard, E. Derat, M. Amatore, C. Aubert, M. Petit, *Org. Lett.* **2016**, *18*, 4242–4245.
- [53] C. Wang, W. J. Teo, S. Ge, *ACS Catal.* **2017**, *7*, 855–863.
- [54] L. Garcia, C. Dinoi, M. F. Mahon, L. Maron, M. S. Hill, *Chem. Sci.* **2019**, *10*, 8108–8118.
- [55] T. K. Mukhopadhyay, M. Flores, T. L. Groy, R. J. Trovitch, *Chem. Sci.* **2018**, *9*, 7673–7680.
- [56] M. Y. Hu, Q. He, S. J. Fan, Z. C. Wang, L. Y. Liu, Y. J. Mu, Q. Peng, S. F. Zhu, *Nat. Commun.* **2018**, *9*, 221–231.
- [57] I. Pappas, S. Treacy, P. J. Chirik, *ACS Catal.* **2016**, *6*, 4105–4109.
- [58] K. L. Lee, *Angew. Chem. Int. Ed.* **2017**, *56*, 3665–3669; *Angew. Chem.* **2017**, *129*, 3719–3723.
- [59] H. L. Sang, S. Yu, S. Ge, *Chem. Sci.* **2018**, *9*, 973–978.
- [60] H. Wen, K. Wang, Y. Zhang, G. Liu, Z. Huang, *ACS Catal.* **2019**, *9*, 1612–1618.
- [61] G. J. Wu, U. Chakraborty, A. Jacobi Von Wangelin, *Chem. Commun.* **2018**, *54*, 12322–12325.
- [62] C. Wu, W. J. Teo, S. Ge, *ACS Catal.* **2018**, *8*, 5896–5900.
- [63] Z. Zong, Q. Yu, N. Sun, B. Hu, Z. Shen, X. Hu, L. Jin, *Org. Lett.* **2019**, *21*, 5767–5772.
- [64] M. Y. Hu, J. Lian, W. Sun, T. Z. Qiao, S. F. Zhu, *J. Am. Chem. Soc.* **2019**, *141*, 4579–4583.
- [65] C. Wang, W. J. Teo, S. Ge, *Nat. Commun.* **2017**, *8*, 2258–2266.
- [66] M. W. Gribble, M. T. Pirnot, J. S. Bandar, R. Y. Liu, S. L. Buchwald, *J. Am. Chem. Soc.* **2017**, *139*, 2192–2195.
- [67] A. M. Tondreau, C. C. H. Atienza, J. M. Darmon, C. Milsmann, H. M. Hoyt, K. J. Weller, S. A. Nye, K. M. Lewis, J. Boyer, J. G. P. Delis, E. Lobkovsky, P. J. Chirik, *Organometallics* **2012**, *31*, 4886–4893.
- [68] X. Q. Jia, Z. Huang, *Nat. Chem.* **2016**, *8*, 157–161.
- [69] A. J. Challinor, M. Calin, G. S. Nichol, N. B. Carter, S. P. Thomas, *Adv. Synth. Catal.* **2016**, *358*, 2404–2409.
- [70] C. H. Schuster, T. Diao, I. Pappas, P. J. Chirik, *ACS Catal.* **2016**, *6*, 2632–2636.
- [71] J. R. Carney, B. R. Dillon, L. Campbell, S. P. Thomas, *Angew. Chem. Int. Ed.* **2018**, *57*, 10620–10624; *Angew. Chem.* **2018**, *130*, 10780–10784.
- [72] B. Raya, S. Jing, T. V. RajanBabu, *ACS Catal.* **2017**, *7*, 2275–2283.
- [73] X. X. Yang, C. Y. Wang, *Angew. Chem. Int. Ed.* **2018**, *57*, 923–928; *Angew. Chem.* **2018**, *130*, 935–940.
- [74] M. Kamitani, H. Kusaka, H. Yuge, *Chem. Lett.* **2019**, *48*, 1196–1198.
- [75] B. Cheng, P. Lu, H. Y. Zhang, X. P. Cheng, Z. Lu, *J. Am. Chem. Soc.* **2017**, *139*, 9439–9442.
- [76] J. Guo, X. Z. Shen, Z. Lu, *Angew. Chem. Int. Ed.* **2017**, *56*, 615–618; *Angew. Chem.* **2017**, *129*, 630–633.
- [77] B. Cheng, W. B. Liu, Z. Lu, *J. Am. Chem. Soc.* **2018**, *140*, 5014–5017.
- [78] X. Du, Y. Zhang, D. Peng, Z. Huang, *Angew. Chem. Int. Ed.* **2016**, *55*, 6671–6675; *Angew. Chem.* **2016**, *128*, 6783–6787.
- [79] D. G. Kong, B. W. Hu, D. F. Chen, *Chem. Asian J.* **2019**, *14*, 2694–2703.
- [80] S. C. Zhang, J. J. Ibrahim, Y. Yang, *Org. Lett.* **2018**, *20*, 6265–6269.
- [81] J. Guo, Z. Lu, *Angew. Chem. Int. Ed.* **2016**, *55*, 10835–10838; *Angew. Chem.* **2016**, *128*, 10993–10996.
- [82] J. Guo, H. L. Wang, S. P. Xing, X. Hong, Z. Lu, *Chem-US* **2019**, *5*, 881–895.
- [83] H. A. Wen, X. L. Wan, Z. Huang, *Angew. Chem. Int. Ed.* **2018**, *57*, 6319–6323; *Angew. Chem.* **2018**, *130*, 6427–6431.
- [84] Z. Q. Zuo, J. Yang, Z. Huang, *Angew. Chem. Int. Ed.* **2016**, *55*, 10839–10843; *Angew. Chem.* **2016**, *128*, 10997–11001.
- [85] W. J. Teo, C. Wang, Y. W. Tan, S. Ge, *Angew. Chem. Int. Ed.* **2017**, *56*, 4328–4332; *Angew. Chem.* **2017**, *129*, 4392–4396.
- [86] M. Kidonakis, M. Stratakis, *Org. Lett.* **2015**, *17*, 4538–4541.
- [87] D. Shao, Y. Li, *RSC Adv.* **2018**, *8*, 20379–20393.
- [88] T. Galeandro-Diamant, R. Sayah, M. L. Zanota, S. Marrot, L. Veyre, C. Thieuleux, V. Meille, *Chem. Commun.* **2017**, *53*, 2962–2965.

- [89] V. Pandarus, R. Ciriminna, G. Gingras, F. Béland, S. Kaliaguine, M. Pagliaro, *Green Chem.* **2019**, *21*, 129–140.
- [90] L. M. Li, Y. X. Li, J. C. Yan, H. Cao, D. Y. Shao, J. J. Bao, *Rsc Adv.* **2019**, *9*, 12696–12709.
- [91] H. C. Zai, Y. Z. Zhao, S. Y. Chen, L. Ge, C. F. Chen, Q. Chen, Y. J. Li, *Nano Res.* **2018**, *11*, 2544–2552.
- [92] Y. Chen, S. Ji, W. Sun, W. Chen, J. Dong, J. Wen, J. Zhang, Z. Li, L. Zheng, C. Chen, Q. Peng, D. Wang, Y. Li, *J. Am. Chem. Soc.* **2018**, *140*, 7407–7410.
- [93] Y. Zhu, T. Cao, C. Cao, J. Luo, W. Chen, L. Zheng, J. Dong, J. Zhang, Y. Han, Z. Li, C. Chen, Q. Peng, D. Wang, Y. Li, *ACS Catal.* **2018**, *8*, 10004–10011.
- [94] K. Motokura, K. Maeda, W.-J. Chun, *ACS Catal.* **2017**, *7*, 4637–4641.
- [95] B. B. Sarma, J. Kim, J. Amsler, G. Agostini, C. Weidenthaler, N. Pfander, R. Arenal, P. Concepcion, P. Plessow, F. Studt, G. Prieto, *Angew. Chem. Int. Ed.* **2020**, *59*, 5806–5815; *Angew. Chem.* **2020**, *132*, 5855–5864.
- [96] I. Buslov, F. Song, X. Hu, *Angew. Chem. Int. Ed.* **2016**, *55*, 12295–12299; *Angew. Chem.* **2016**, *128*, 12483–12487.
- [97] T. Galeandro-Diamant, I. Suleimanov, L. Veyre, M. Bousquie, V. Meille, C. Thieuleux, *Catal. Sci. Technol.* **2019**, *9*, 1555–1558.
- [98] Z. K. Zhang, L. C. Bai, X. L. Hu, *Chem. Sci.* **2019**, *10*, 3791–3795.
- [99] Y. B. Zhou, Z. K. Liu, X. Y. Fan, R. H. Li, G. L. Zhang, L. Chen, Y. M. Pan, H. T. Tang, J. H. Zeng, Z. P. Zhan, *Org. Lett.* **2018**, *20*, 7748–7752.
- [100] R. H. Li, X. M. An, Y. Yang, D. C. Li, Z. L. Hu, Z. P. Zhan, *Org. Lett.* **2018**, *20*, 5023–5026.
- [101] T. Mitsudome, S. Fujita, M. Sheng, J. Yamasaki, K. Kobayashi, T. Yoshida, Z. Maeno, T. Mizugaki, K. Jitsukawa, K. Kaneda, *Green Chem.* **2019**, *21*, 4566–4570.
- [102] L. Cao, Z. Lin, F. Peng, W. Wang, R. Huang, C. Wang, J. Yan, J. Liang, Z. Zhang, T. Zhang, L. Long, J. Sun, W. Lin, *Angew. Chem. Int. Ed.* **2016**, *55*, 4962–4966; *Angew. Chem.* **2016**, *128*, 5046–5050.
- [103] R. Azuma, S. Nakamichi, J. Kimura, H. Yano, H. Kawasaki, T. Suzuki, R. Kondo, Y. Kanda, K.-i. Shimizu, K. Kato, Y. Obora, *ChemCatChem* **2018**, *10*, 2378–2382.
- [104] J. W. Zhang, G. P. Lu, C. Cai, *Green Chem.* **2017**, *19*, 2535–2540.
- [105] J. Wen, Y. Chen, S. Ji, J. Zhang, D. Wang, Y. Li, *Nano Res.* **2019**, *12*, 2584–2588.
- [106] H. Miura, K. Endo, R. Ogawa, T. Shishido, *ACS Catal.* **2017**, *7*, 1543–1553.

Manuscript received: June 22, 2020

Accepted manuscript online: July 15, 2020

Version of record online: December 1, 2020